

This is an Open Access document downloaded from ORCA, Cardiff University's institutional repository: <https://orca.cardiff.ac.uk/id/eprint/120611/>

This is the author's version of a work that was submitted to / accepted for publication.

Citation for final published version:

Abdullah, Isam, Lan, He, Morrison, John, Alharbi, Ahmed, Macdonald, J. Emyr and Yeates, Stephen G. 2018. The synergistic role of azeotropic solvent mixtures and atactic polystyrene on the morphology, crystallization and field effect mobility of thin film 6,13-bis (triisopropylsilylethynyl)-pentacene based semiconductors. *Journal of Materials Science: Materials in Electronics* 29 (12) , pp. 9804-9813. 10.1007/s10854-018-9020-5

Publishers page: <http://dx.doi.org/10.1007/s10854-018-9020-5>

Please note:

Changes made as a result of publishing processes such as copy-editing, formatting and page numbers may not be reflected in this version. For the definitive version of this publication, please refer to the published source. You are advised to consult the publisher's version if you wish to cite this paper.

This version is being made available in accordance with publisher policies. See <http://orca.cf.ac.uk/policies.html> for usage policies. Copyright and moral rights for publications made available in ORCA are retained by the copyright holders.



The synergistic role of azeotropic solvent mixtures and atactic polystyrene on the morphology, crystallization and field effect mobility of thin film 6,13-bis(triisopropylsilylethynyl-pentacene based semiconductors

Isam Abdullah^a, He Lan,^b John Morrison,^b Ahmed Alharbi,^b J Emyr Macdonald^a and Stephen G. Yeates^{b,*}

(a) School of Physics and Astronomy, Cardiff University, The Parade, Cardiff CF24 3AA, U.K.

(b) Organic Materials Innovation Centre (OMIC), School of Chemistry, The University of Manchester, M13 9PL, Manchester, United Kingdom.

(*) To whom correspondence should be addressed.

Keywords: AFM, TIPS-pentacene, polymer blend, crystallization, solvent blend

Abstract

The effect of anisole / decane binary solvent mixture and the subsequent addition of low wt-% aPS on 6,13-bis(triisopropylsilylethynyl-pentacene (TIPS-pentacene) thin film morphology is investigated by optical microscopy, AFM and UV-vis measurements. We show that, over the composition range anisole/decane of 96/4 to 85/15 wt-%, the solution maintains an azeotropic composition with the boiling point of the binary mixture remaining constant at 152 °C, and the solvent composition remaining constant during evaporation and drying. It was found that addition of up to 20 wt-% decane has little impact on micro-scale crystal morphology but has a significant influence on the growth mode and terrace roughness. The formation of large crystals is explained in terms of the change in solvent, increase in decane content, weakening the solute-solvent interactions and promoting efficient nucleation of the favoured H-aggregates of TIPS-pentacene. The effect of the TIPS-pentacene - aPS ratio up to 20 wt-% for drop-cast thin film was similarly investigated. It is found that addition of aPS has a significant effect on both macroscopic crystal properties such as surface coverage, unity of orientation and long range order. It also changes the surface morphology and layer ordering on the nano-scale.

1. INTRODUCTION

Whilst the highest charge carrier mobilities in small molecule organic semi-conductors (OSC) have been obtained from single crystal studies [1], the performance of solution grown crystalline thin films have improved dramatically over recent years [2,3]. These improvements in Organic Field Effect Transistor ((OFET) device performance have been brought about in the main by a greater understanding on the role of morphology and molecular alignment in the charge transfer efficiency of thin films [4-7]. Morphology control strategies for solution processing OSC thin films have recently been reviewed [8], with a focus on three distinct aspects: control of nucleation, crystal growth, and domain alignment, with particular emphasis on methods that exploit the unique characteristics of solution processing.

6,13-bis(triisopropylsilylethynyl-pentacene (TIPS-pentacene) has become a standard high performance OSC and there is a wealth of recent studies showing how formulation [9-11] and process parameters [12-14] can give rise to organic field effect hole mobilities (μ_{FET}) which can vary over several orders of magnitude. Notably, appropriate solvent mixtures have been shown to significantly improve device performance and reproducibility [15,16]. In this paper we focus on the effect of binary solvent mixtures on the morphology and crystallisation of TIPS-pentacene thin films. We then go on to consider the previously unreported addition of low volume fraction of electronically inert amorphous atactic polystyrene [16-19] both on clean silicon and on silicon treated with polyvinyl pyrrolidone (PVP).

2. EXPERIMENTAL SECTION

TIPS-pentacene was synthesized according to the Swager modification of the Anthony method [20]. Methoxybenzene (anisole, anhydrous 99%, bpt = 153.8 °C), decane (anhydrous \geq 99%, bpt = 174 °C) and amorphous atactic polystyrene (aPS, M_w = 900 kDa), poly(melamine-*co*-formaldehyde) methylated (solution average M_n ~432, 84 wt-% in 1-butanol) and poly(4-vinylphenol) (PVP, M_w ~11,000) were all obtained from Sigma-Aldrich UK and used as received.

TIPS-pentacene – aPS solution blends were prepared as follows. Stock solutions (2 wt-% in solvent) of TIPS-pentacene and aPS were prepared. TIPS-pentacene stock solution was filtered

using a 0.45 μm PTFE filter. aPS binder solutions were left unfiltered. Blends were prepared fresh prior to device fabrication, with a total mass content of 2 wt-%.

For solvent evaporation, 10 mL solutions of 5 and 10 % v/v (96/4 and 93/7 wt-%) decane in anisole were prepared and shaken to homogenise. 10 drops (60 μL) were applied to a single spot on a clean glass slide and allowed to evaporate at room temperature. At 3 minute intervals, 6 μL aliquots of the solution was withdrawn by pipette and sealed in NMR tubes with 600 μL of deuterated chloroform. This was continued over evaporation till less than 6 μL remained, at which point the thin film of residual solvent was taken up in chloroform-*d* and sealed in a NMR tube. On both runs this degree of evaporation was observed on the 7th measurement at 18 mins. Proton NMR spectra were recorded at 400 MHz on a Bruker Advance III HD instrument with cryoprobe. Data was processed on ACD/Labs academic edition software.

Discrete bottom-gate, top-contact organic field effect transistor (OFET) devices were fabricated on heavily n-doped silicon wafers comprising a 3000 \AA thermally grown gate oxide layer. Substrates were cleaned by sonication in de-ionised water for 15 minutes, then acetone for 15 minutes and finally methanol for 15 minutes. Substrates were then dried on a hot plate for 2 hours at 150 $^{\circ}\text{C}$ under normal atmosphere. An organic gate dielectric consisting of 3.4 wt% polyvinyl pyrrolidone (PVP) and 1.1 wt% of poly(melamine-co-formaldehyde) in propylene glycol monomethyl ether acetate (PGMEA) solution was then spin coated at 2000 rpm for a duration of 30 secs. Substrates were then dried on a hot plate for 2 mins at 120 $^{\circ}\text{C}$ and cured under normal atmosphere at 160 $^{\circ}\text{C}$ for 30 mins [1]. Appropriate TIPS-pentacene solution were then drop cast at 30 $^{\circ}\text{C}$ onto the wafer tilted at 5 $^{\circ}$ and allowed to dry for three hours, yielding on average 100nm dry thick films. Gold source and drain channel electrodes, 60 μm width and 2 mm length were thermally evaporated, at 10^{-6} mBar at a rate of 0.1 nm/s for the first 10 nm and then 0.3 nm/s until a layer thickness of 50 nm was obtained, yielding 9 transistors per substrate. Devices were characterized in DC current using an E5270B 8Slot precision Measurement frame from Agilent Technology coupled to a 3 Agilent E5287A atto level High Resolution Module. Contacts were made using Karl Süss PH100 manual microprobes. Contacts were made using Karl Süss PH100 manual microprobes. To remain in the saturated regime, the value of the drain voltage was kept equal to the gate voltage at all times. From the slope of the square root of the drain intensity characteristic, we were able to

calculate the saturated hole mobility (μ_{FET}) and the threshold voltage, according to the following equation:

$$I_D = \frac{\mu_{FET} W C_i}{2L} (V_G - V_T)^2 \quad (1)$$

where W is the width of the channel (60 μm), L the length of the channel (2mm), C_i is the equivalent capacitance of the dielectric intercepting the channel and V_T the threshold voltage. Measurements were performed in dark ambient conditions.

Thin films for optical and atomic force microscopy studies were prepared as follows. Heavily n-doped silicon wafers comprising a 3000 Å thermally grown gate oxide layer were cleaned by sonication in de-ionised water for 15 mins, then acetone for 15 mins and finally methanol for 15 mins. Substrates were then dried on a hot plate for 2 hrs at 150 °C under normal atmosphere. Where appropriate an organic gate dielectric consisting of 3.4 wt-% polyvinyl pyrrolidone (PVP) and 1.1 wt-% of poly(melamine-co-formaldehyde) in propylene glycol monomethyl ether acetate (PGMEA) solution was then spin coated at 2000 rpm for a duration of 30 secs. Substrates were then dried on a hot plate for 2 mins at 120 °C and cured under normal atmosphere at 160 °C for 30 mins [22]. Appropriate TIPS-pentacene solution were then drop-cast at 30 °C onto the wafer tilted at 5° and allowed to dry for three hours.

Atomic force microscopy (AFM) imaging was performed using a Bruker Multimode system in intermittent contact mode using standard silicon tips.

UV-vis spectra were obtained on a Nicolet Evolution 300 spectrometer using 1 cm quartz cells at a constant concentration of 1×10^{-5} M.

3. RESULTS AND DISCUSSION

It has previously been reported that TIPS-pentacene OFET devices deposited from miscible binary solvent mixtures of anisole with low weight fraction of decane in a discrete bottom-gate, top-contact organic field effect transistor configuration utilising an organic gate dielectric comprising polyvinyl pyrrolidone (PVP) crosslinked with poly(melamine-co-formaldehyde) [21] have significantly improved device to device characteristics when compared with either pure anisole or decane alone [16]. To date the nature of miscible binary solvent mixtures of anisole with low weight fraction of decane has not been disclosed.

Li et al[15] have previously shown that utilising the azeotropic behaviour of miscible binary mixtures of isopropanol (polar, poor solvent, bpt 82.6 °C) and toluene (apolar, good solvent, bpt = 153.8 °C) nucleation and growth of TIPS-pentacene crystals from solution can be controlled. Upon drop casting TIPS-pentacene from a solvent mixture at a polar component concentrations just higher than that of the azeotropic point (e.g. IPA/toluene > 50.1/49.9 %v/v) predominantly parallelepiped single crystals with length and width of up to 2 mm and 700 μm respectively are facily self-assembled in a well-controlled manner. The formation of large crystals is explained in terms of the change in solvent, increase in alcohol content, weakening the solute-solvent interactions and promoting efficient nucleation of the favoured H-aggregates of TIPS-pentacene.

We have found no literature precedent for an anisole/decane azeotrope and so conducted a simple test to check for depression of boiling point in mixtures of these solvents. For TIPS-pentacene the rank order of the goodness of solvent expressed by interaction radius, R_a , is toluene, anisole, decane and isopropanol (R_a is calculated as 2.2, 5.3, 7.0 and 16.3 $\text{MPa}^{1/2}$ respectively)[23]. UV/vis of anisole/decane mixtures, Figure 1, show a blue shift with increasing decane content supporting enhanced supramolecular H-aggregate formation [24,25].

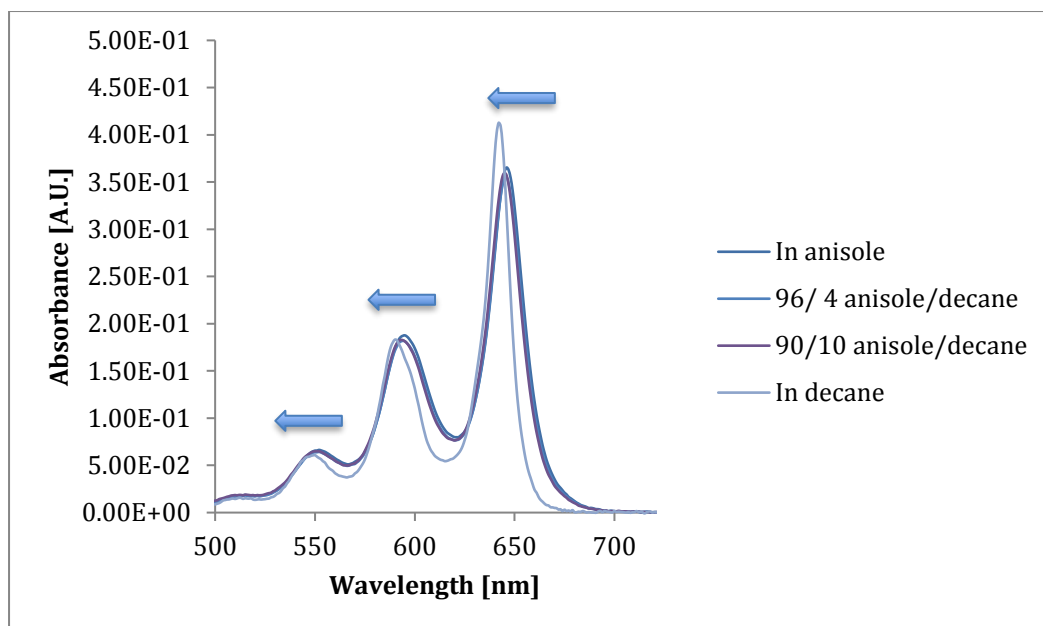


Figure 1. UV/Vis absorption spectra of TIPS-pentacene dissolved in different anisole/decane solvent mixtures at a constant 1×10^{-5} M. Arrows illustrate the blue shift with increasing decane content.

Over the composition range anisole/decane of 96/4 to 85/15 wt-% the boiling point of the binary mixture remained constant at 152 °C. Comparison of the composition of the first few millilitres of distillate, carried out using the ^1H NMR integral for the anisole PhOCH_3 3H singlet at $\delta = 3.83$ ppm standardised to 100 and the integral for the decane 6H CH_3 triplet at $\delta = 0.90$ ppm, showed that over the entire range the composition of the distillate mirrored fairly closely that of the initial solvent mixture. To check whether an increase in decane concentration occurs on evaporation of the solvent mixture, a small quantity of the solvent mixtures anisole/decane ratios of 96/4 and 93/7 wt-% was applied to a glass slide and allowed to evaporate under ambient conditions while being sampled and examined by NMR until > 80% solvent evaporation, Table 1. We see that over the anisole/decane composition range examined, close to azeotropic behavior is observed.

Table 1: NMR integral % for the decane CH_3 triplet at $\delta = 0.90$ ppm vs anisole singlet at $\delta = 3.83$ ppm for the two solutions evaporating over time.

T (min)	0	3	6	9	12	15	18
4 wt-% decane	5.9	5.9	5.8	5.7	5.4	5.0	4.1
7 wt-% decane	12.8	12.4	12.2	12.6	12.0	11.6	11.6

Table 2 shows OFET devices deposited from miscible binary solvent mixtures of anisole with low weight fraction of decane in a discrete bottom-gate, top-contact organic field effect transistor configuration utilizing an organic gate dielectric comprising polyvinyl pyrrolidone (PVP) cross-linked with poly(melamine-co-formaldehyde) [21]. Over the azeotropic range we find both improved device yield and maximum μ_{FET} at 93/7 wt-% anisole/decane.

Table 2. Charge carrier mobility of TIPS-pentacene field-effect transistors at different solvent ratios (average 9 devices).

Ratio anisole/decane (wt-%)	100/0	96/4	93/7	92/8	89/11	85/15
% working devices	78	78	100	100	100	78
Average μ_{FET} (excluding non-working devices) cm^2/Vs	0.014	0.011	0.08	0.013	0.014	0.004
Maximum μ_{FET} (excluding non-working devices) cm^2/Vs	0.036	0.027	0.16	0.025	0.034	0.021
Minimum μ_{FET} (excluding non-working devices) cm^2/Vs	0.0003	0.0009	0.012	0.002	0.0003	0.00003
On/Off ratio	$10^3 - 10^4$	10^4	$10^3 - 10^4$	10^4	$10^3 - 10^4$	$10^2 - 10^3$

3.1 Influence of anisole/decane ratio on TIPS-pentacene on crystal growth and surface roughness of TIPS-pentacene. In order to gain insight into the crystal growth of TIPS-pentacene from anisole/decane, binary mixtures, solutions were drop cast onto SiO₂ tilted at 5° since this has been shown to result in an array of ribbon shaped TIPS-pentacene crystals well-aligned in the direction of tilt [26]. Optical microscopy, shown in Figure 2, shows needle like crystals, with widths ranging from 50 to several hundred of microns, with voids regions between the crystals, across the entire solvent blend range.

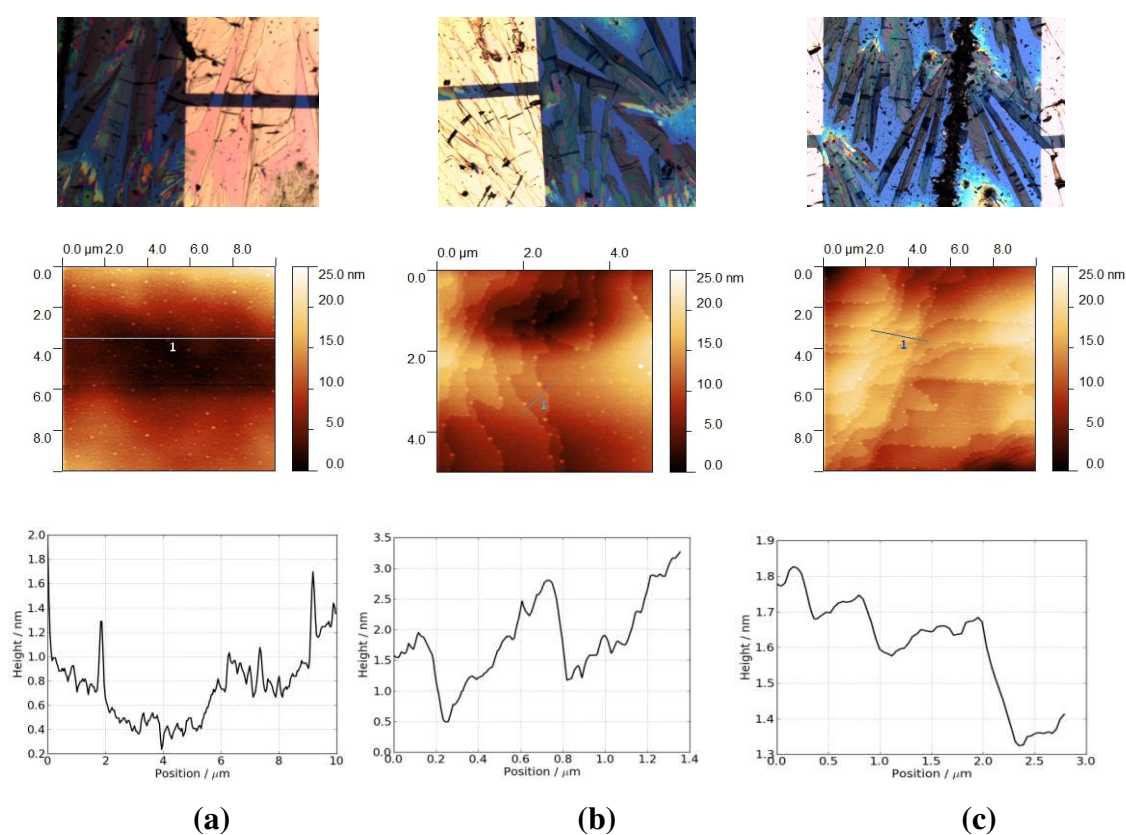


Figure 2. TIPS-pentacene as a function of anisole/decane wt-% ratio. (a) pure anisole, (b) anisole/decane 96/4 wt-%, (c) anisole/decane 90/10 wt-%. Top: Optical image with the golden areas showing vacuum-deposited gold electrodes, channel length 60 μm. Middle: AFM images for which the numbered sections are shown in the corresponding bottom panel.

For TIPS-pentacene in pure anisole, AFM shows films of roughness 6.3 ± 2.2 nm with grain-like nanodots of the order of 30 nm in lateral dimensions, Figure 2a. The introduction of decane to the solvent induces significant changes to the surface. Figure 2b shows the morphology for

an anisole/decane ratio of 96/4 wt-% which is dominated by stepped terraces which were not apparent for pure anisole solvent. The step edges are wavy rather than straight and are decorated with grain-like nanodots of around 46 ± 5 nm lateral dimensions with similar behavior observed at higher decane ratios, Figure 2c. It is unclear whether the presence of these nanodots strongly affects the step waviness: in some images the waviness correlates clearly with the presence of nanodots and elsewhere nanodots occur at relatively straight terrace steps. Similar terraces decorated with such nanodots have been reported for TIPS-pentacene films deposited from chloroform solution by confined solution deposition with a PFPE stamp [27]. The formation of ordered terraces strongly indicates step-flow crystalline growth. Step heights deduced from line profiles are 1.6 nm and 3.5 ± 0.1 nm, consistent with the c-axis spacing of 1.54 nm in the triclinic unit cell of TIPS-pentacene. Smaller step heights of around 1.4 nm were also observed, which may correspond to a tilted molecular orientation. The occurrence of the nanodots at the step edges indicates that these comprise impurities expelled by the growing step front as previously suggested [27]. For these compositions, the overall surface roughness is of the order of 2 - 5 nm, depending on the step density. The roughness of the flat terraces between the steps is lower and is sensitive to solvent ratio, showing a clear minimum at 7-8 anisole/decane wt-%t, as shown in Figure 3a.

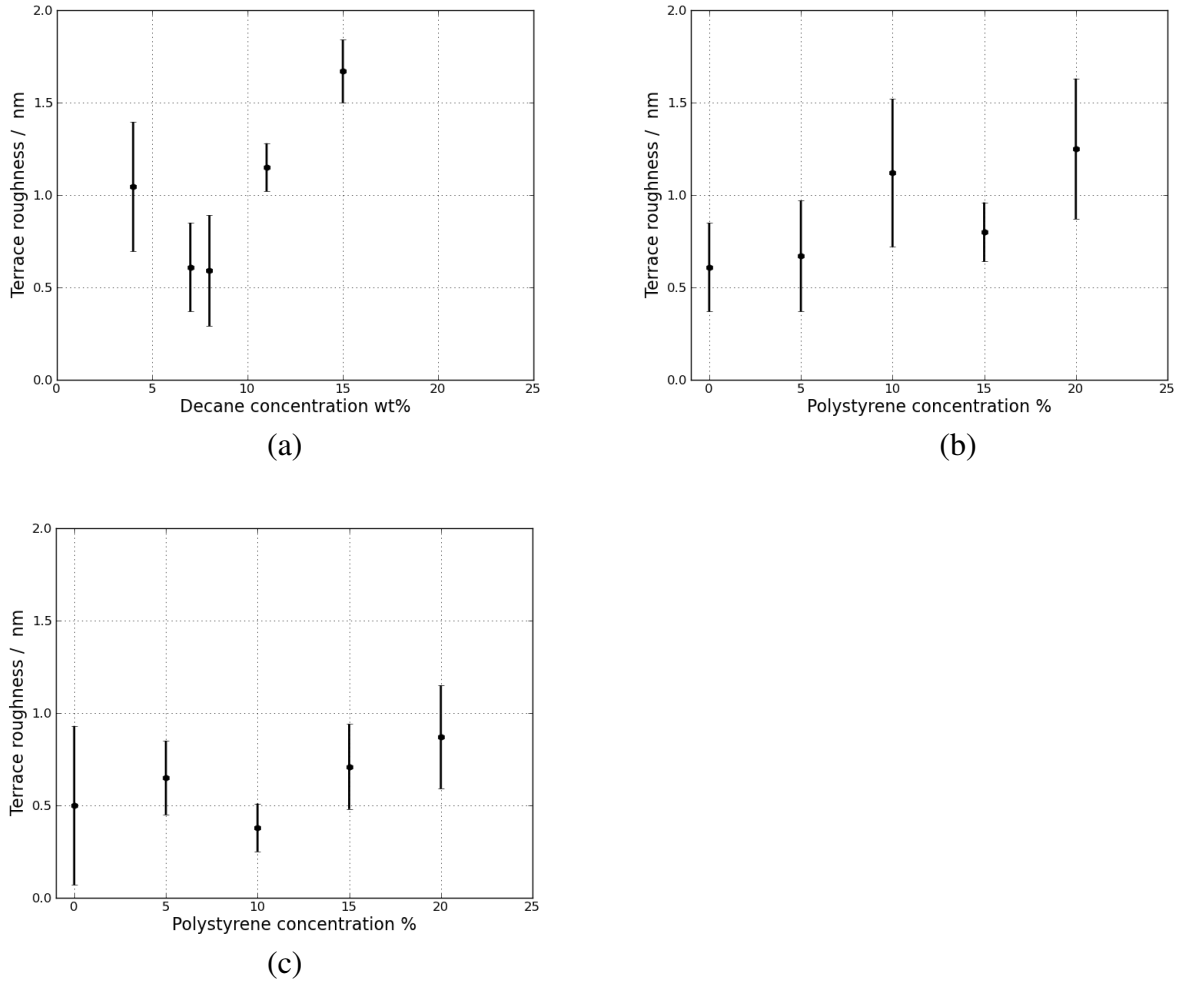


Figure 3. The surface roughness on top of terraces of TIPS-pentacene for (a) varying composition of anisole/decane binary solvent on silicon (b) varying aPS concentration for 93/7 wt-% anisole/decane solvent on silicon (c) the same conditions as (b) for films deposited onto PVP-treated silicon.

3.2 Influence of low concentration of polystyrene on OFET performance, crystal growth,

morphology and surface roughness of TIPS-pentacene.

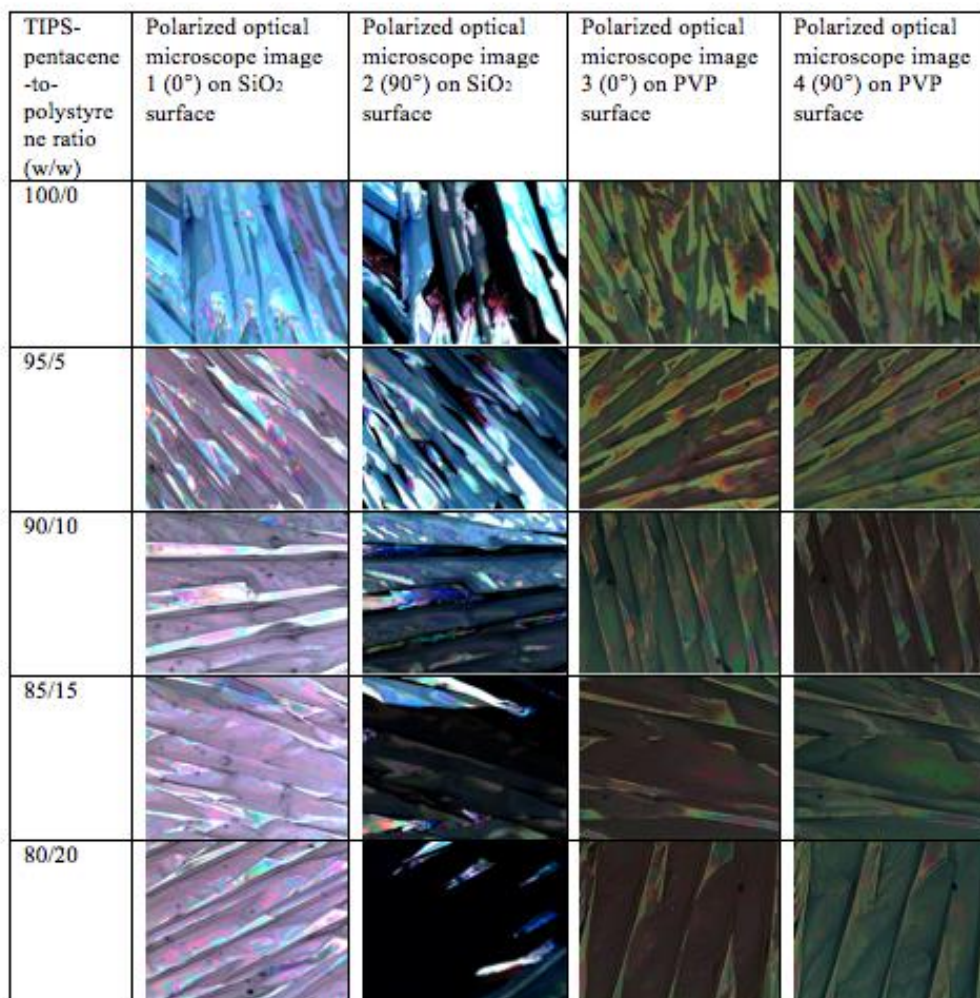
The effect of formulation was further considered by the addition of a low weight fraction of atactic polystyrene to 93/7 wt-% anisole/decane. as this was shown to the highest combination of μ_{FET} and device yield (Table 2). Atactic polystyrene (aPS) was chosen as it has previously been shown to give rise to a slight increase in device performance over pure TIPS-pentacene but more importantly an increase in device uniformity [18-19]. In Table 3 we see that the addition of low wt-% atactic polystyrene gives both a increase in average and maximum μ_{FET} with retention of 100% device yield.

Table 3: Charge carrier mobility of TIPS-pentacene field-effect transistors at different TIPS-pentacene to polystyrene ratio in 93/7 wt-% anisole/decane (average of 9 devices, 100% yield)

Ratio TIPS-pentacene - aPs wt-%	100/0	95/5	90/10	85/15	80/20
Average μ_{FET} (excluding non-working devices) cm^2/Vs	0.08	0.14	0.17	0.15	0.14
Maximum μ_{FET} (excluding non-working devices) cm^2/Vs	0.16	0.48	0.25	0.45	0.23
Minimum μ_{FET} (excluding non-working devices) cm^2/Vs	0.012	0.001	0.04	0.01	0.05
On/Off ratio	$10^3 - 10^4$	10^4	$10^3 - 10^4$	10^4	$10^3 - 10^4$

As polystyrene content increases we observe that not only the crystal plates become more aligned, but also that surface coverage improves with almost the entire surface covered at a 85:15 wt-% TIPS-pentacene - aPS ratio, Figure 4.. Moreover, since TIPS-pentacene absorbs polarized light most strongly when the light is aligned with the conjugated pentacene stack, the difference between brightness under polarized optical microscope is indicative of a different degree of long-range order of TIPS-pentacene stacking. The brightness change becomes sharper and the regions of uniform color become larger as the amount of polystyrene increases, indicating that the addition of aPS not only improves surface coverage but also promotes micro-scale long-range order. The corresponding effect of blending with aPS at the nanoscale morphology was probed with as a function of TIPS-pentacene - aPS ratio using AFM in intermittent-contact mode, Figure 5.

Figure 4. Large area optical images of drop cast TIPS-pentacene polystyrene blends crystals grown on both SiO₂ and poly(vinyl phenol) surfaces. drop cast TIPS-pentacene - aPS blends in 2 wt-% in 93/7 wt-% anisole/decane,



On SiO₂ substrates, AFM images reveal step heights of 1.6 nm, which corresponds to the pentacene molecule length. This result demonstrates that the pentacene conjugated axis is close to perpendicular to the SiO₂ substrate surface, Figure 5. Similar stepped surfaces with flat terraces are observed across samples with different aPS compositions, but two differences are apparent: the step edges are much straighter than those for pristine TIPS-pentacene and larger nanodots, of the order of 125 nm or more across, are observed on the terraces between steps. These nanodots observed on terraces in Figure 5 are likely to be rich in aPS. Here the terrace roughness is similar to that without PS, Figure 3a, and the effect of increasing aPS concentration is weak, as seen in Figure 3b.

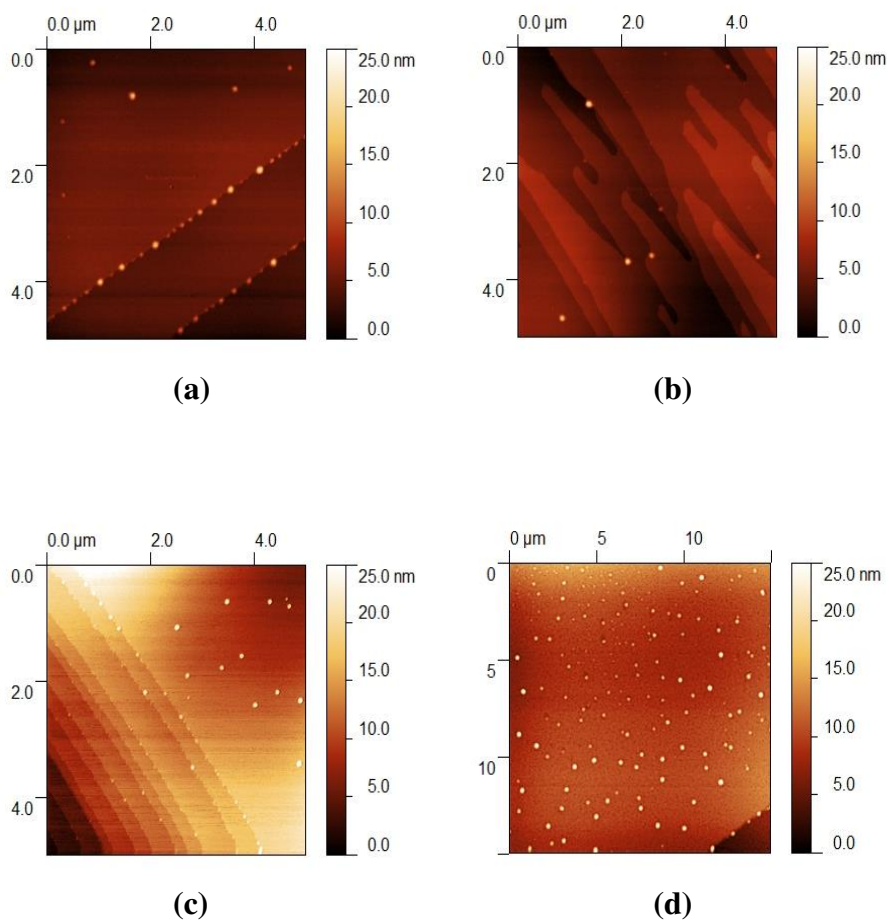


Figure 5. AFM images (5 μm scan size) of TIPS-pentacene blended with aPS drop cast from 93/7 wt-% anisole/decane on SiO_2 at 30 $^\circ\text{C}$ (a) 5 wt-% aPS, (b) 10 wt-% aPS, (c) 15 wt-% aPS and (d) 20 wt-% aPS.

AFM images of TIPS-pentacene films deposited onto PVP dielectric films on silicon, Figure 6, revealed the distribution of single and multi-layered TIPS-pentacene islands, again consistent with step-flow growth of incomplete monolayers. The island heights are in the range 1.60 to 1.75 nm, again consistent with the (001) spacing.

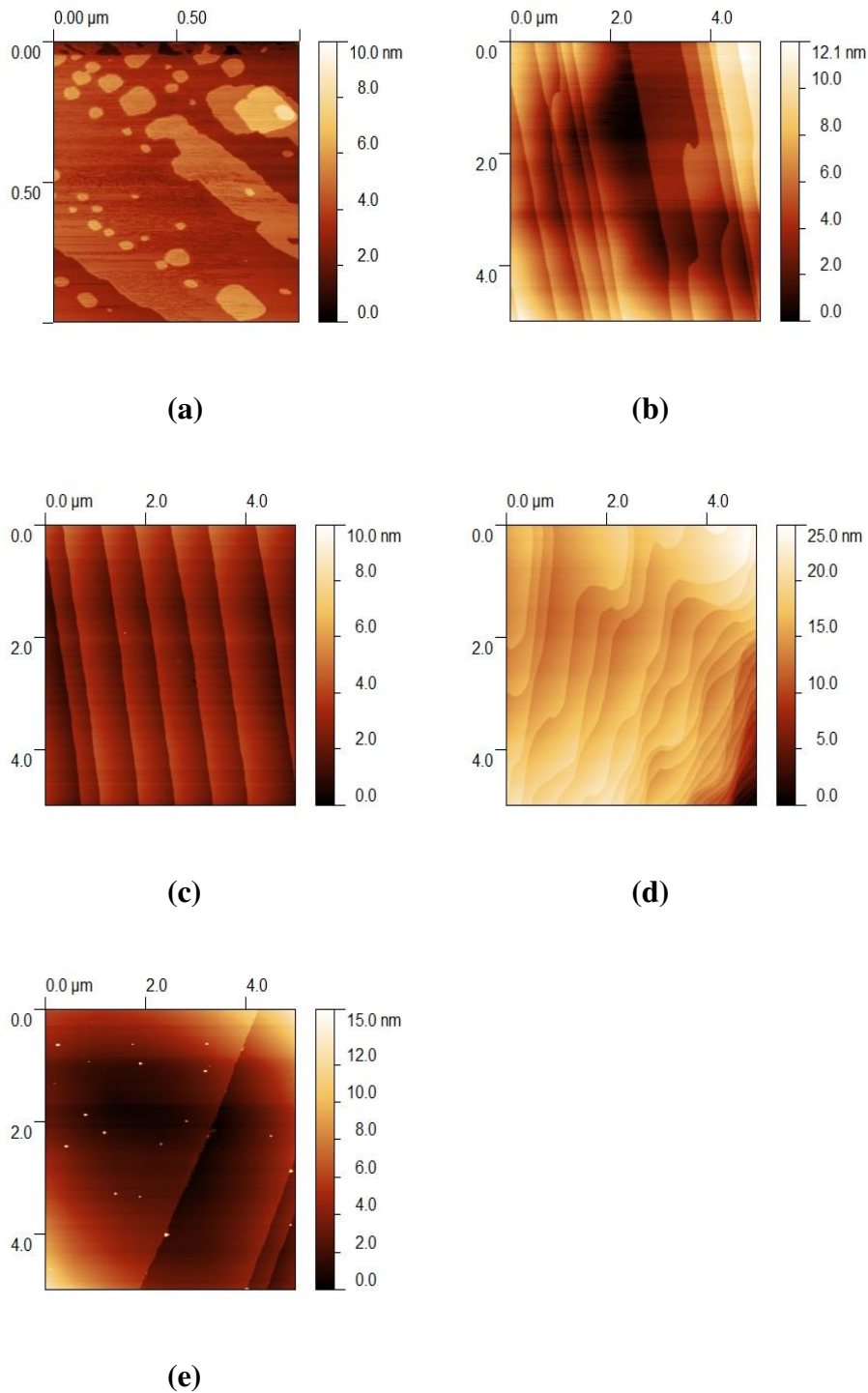


Figure 6. AFM images of pure and blended TIPS-pentacene from drop casted from 93/7 wt-% anisole/decane on PVP at 30 °C. (a) pure TIPS-pentacene, (b) 5 wt-% aPS, (c) 10 wt-% aPS, (d) 15 wt-% aPS, (e) 20 wt-% aPS .

The addition of 5 wt-% aPS leads to completely disappearing of scattered nanodots in AFM images and replaced with well-defined ordered but wavy terraces which is not observed in pure TIPS-P on PVP. As the aPS content is increased to 10 wt-%, the crystal size is further enlarged

and the terraces become more regular and straight. The step edges are straight over several areas imaged for 10 wt-% aPS whereas they are wavier at higher aPS concentrations. A particularly noticeable difference for the PVP-covered silicon substrate is the absence of nanodots on the terraces or at step edges for aPS compositions up to 15 wt-%. Some nanodots, likely to consist of un-incorporated aPS, are apparent at 20 wt-%. This difference from the clean silicon oxide surface is believed to be related to the low surface energy of PVP, 34.2 mJ m^{-2} , favoring adhesion of hydrophobic groups [28]. Additionally, the roughness of the terraces is marginally lower than for corresponding films grown directly onto the silicon surface.

4. Conclusion

Over the composition range anisole/decane of 96/4 to 85/15 wt-% the boiling point of the binary mixture remains constant at $152 \text{ }^{\circ}\text{C}$, and the composition fairly constant during evaporation and drying. The effect of anisole/decane solvent mixture over this range for drop-casted TIPS-pentacene thin film is investigated by optical microscopy, AFM and UV-vis measurements. It was found that addition of up to 20 wt-% decane has no impact on micro-scale crystal morphology but has a significant influence on both mean size of nanodots and average surface roughness. It promotes step-flow growth leading to flat terraces of mean surface roughness of 1 nm or less surrounded by well-defined steps corresponding to the c-axis molecular spacing. The formation of large crystals is explained in terms of the change in solvent, increase in decane content, weakening the solute-solvent interactions and promoting efficient nucleation of the favoured H-aggregates of TIPS-pentacene. The effect of the TIPS-pentacene - aPS ratio up to 20 wt-% for drop-cast thin film was similarly investigated. It is found that addition of aPS has a significant effect on macroscopic crystal properties such as surface coverage, unity of orientation and long range orders and surface morphology and layer ordering on the nano-scale. Growth of films on PVP-treated silicon, of low surface energy, leads to smooth terraces devoid on nm-sized nanodots.

Acknowledgements

JM was in part supported by funding from the Engineering and Physical Sciences Research Council (UK) via a Flagship Grant (FS/01/01/10) from the Innovative electronic-Manufacturing Research Centre, Loughborough. IA thanks the Iraqi Cultural Attache for sponsorship and Salahaddin University for ongoing support. This work was funded by the Engineering and Physical Sciences Research Council (EP/K039547/1). All data accompanying this publication are directly available within the publication and supplemental information.

References

- [1] Y. Yongbo, G. Giri, A. L. Ayzner, A.P. Zoombelt, S.C. B. Mannsfeld, J. Chen, D. Nordlund, M. F. Toney, J.Huang, Z. Bao. Ultra-high mobility transparent organic thin film transistors grown by an off-centre spin-coating method, *Nature Comm.*, **5**, 3005 (2014).
- [2] G.P. Rigas, M. Shkunov, *Solution Processable Organic Single Crystals*, *Polymer Science, Ser. C*, **56**, 20-31, (2014).
- [3] S.K. Gupta, P. Jha, A. Singh, M. M. Chehimi, D.K. Aswal, *Flexible Organic Semiconductor Films*, *J. Mater. Chem. C: Materials for Optical and Electronic Devices*, **3**, 8468-8479 (2015).
- [4] S. Bi, Z. He, J. Chen, D.Li, *Solution-grown small-molecule organic semiconductor with enhanced crystal alignment and areal coverage for organic thin film transistors*, *AIP Advances* **5**, 077170 (2015).
- [5] Y. Fujisaki, D. Takahashi, Y. Nakajima, M. Nakata, H.Tsuji, T. Yamamoto, *Alignment Control of Patterned Organic Semiconductor Crystals in Short-Channel Transistor Using Unidirectional Solvent Evaporation Process*, *IEEE Transactions on Electron Devices*, **62**, 2306-2312 (2015).
- [6] J-F. Chang, T. Sakanoue, Y. Olivier, T. Uemura, M-B. Madec, S.G. Yeates, J. Cornil, J. Takeya, A. Troisi, H. Sirringhaus, *Hall-effect measurements probing the degree of charge-carrier delocalization in solution-processed crystalline molecular semiconductors*. *Phys. Rev. Lett.* **107**, 066601 (2011).
- [7] R.Z. Rogowski, A. Dzwilewski, M. Kemerink, A.A. Darhuber, *Solution Processing of Semiconducting Organic Molecules for Tailored Charge Transport Properties*, *J. Phys. Chem. C*, **115**, 11758–11762 (2011).

- [8] Y. Diao, L. Shaw, Z. Bao, S.C.B. Mannsfeld, Morphology control strategies for solution-processed organic semiconductor thin films *Energy Environ. Sci.*, **7**, 2145-2159 (2014).
- [9] S. S. Lee, C. S. Kim, E. D. Gomez, B. Purushothaman, M. F. Toney, C. Wang, A. Hexemer, J. E. Anthony, Y.-L. Loo, Controlling Nucleation and Crystallization in Solution-Processed Organic Semiconductors for Thin-Film Transistors, *Adv. Mater.*, **21**, 3605-3609 (2009).
- [10] S. S. Lee, S. Muralidharan, A. R. Woll, M. A. Loth, Z. Li, J. E. Anthony, M. Haataja, Y.-L. Loo, Understanding Heterogeneous Nucleation in Binary, Solution-Processed, Organic Semiconductor Thin Films, *Chem. Mater.*, **24**, 2920-2928 (2012).
- [11] G.J. Chae, S.H. Jeong, J.H. Baek, B. Walker, C.K. Song, J.H. Seo, Improved performance in TIPS-pentacene field effect transistors using solvent additives, *J. Mater. Chem. C*, **1**, 4216-4221 (2013).
- [12] H. Minemawari, T. Yamada, H. Matsui, J. Y. Tsutsumi, S. Haas, R. Chiba, R. Kumai and T. Hasegawa, Inkjet Printing of Single Crystal Films, *Nature*, **475**, 364-367 (2011).
- [13] Y. Diao, B. C. K. Tee, G. Giri, J. Xu, D. H. Kim, H. A. Becerril, R. M. Stoltenberg, T. H. Lee, G. Xue, S. C. B. Mannsfeld, Z. N. Bao, Solution coating of large-area organic semiconductor thin films with aligned single-crystalline domains, *Nat. Mater.*, **12**, 665-671 (2013).
- [14] H. Li, B. C. K. Tee, J. J. Cha, Y. Cui, J. W. Chung, S. Y. Lee, Z. Bao, High-Mobility Field-Effect Transistors from Large-Area Solution-Grown Aligned C₆₀ Single Crystals, *J. Am. Chem. Soc.*, **134**, 2760-2765 (2012).
- [15] X. Li, B.K.C. Kjellander, J.E. Anthony, C.W.M. Bastiaansen, D.J. Boer, G.H. Gelinck, Azeotropic binary solvent mixtures for preparation of organic single crystals, *Adv. Func. Mater.*, **19**, 3610-3617 (2009).
- [16] M-B Madec, D. Crouch, David; G.R. Llorente, T.J. Whittle, M. Geoghegan, S.G. Yeates, Organic field effect transistors from ambient solution processed low molar mass semiconductor-insulator blends, *J. Mater. Chem.*, **18**, 3230-3236 (2008).
- [17] M.M. Ibrahim, A.C. Maciel, C.P. Watson, M.-B. Madec, S.G. Yeates, D.M. Taylor, Thermo-mechanical stabilisation of a crystalline organic semiconductor for robust large area electronics, *Organic Electronics*, **11**, 1234-1241 (2010).
- [18] M-B. Madec, P.J. Smith, A. Malandraki, N. Wang, J.G. Korvink, S.G. Yeates, Enhanced reproducibility of inkjet printed organic thin film transistors based on solution processable polymer-small molecule blends, *J. Mater. Chem.*, **20**, 9155-9160 (2010).
- [19] J. Smith, R. Hamilton, Y. Qi, A. Kahn, D.D.C. Bradley, M. Heeney, I. McCulloch,

- T.D. Anthopoulos, The Influence of Film Morphology in High-Mobility Small-Molecule: Polymer Blend Organic Transistors, *Adv. Func. Mat.*, **20**, 2330-2337 (2010).
- [20] Y. Kim, J. E. Whitten, T. M. Swager, High Ionization potential conjugated polymers, *J. Am. Chem. Soc.* **127**, 12122–12130 (2005).
- [21] S.K Park, T.N. Jackson, J.E. Anthony, D.A. Mourey, High mobility solution processed 6,13-bis(triisopropyl-silylethynyl)pentacene organic thin film transistors. *Appl. Phys. Lett.* **91**, 063514 (2007).
- [22] J. E. Anthony, J. S. Brooks, D. L. Eaton, S. R. Parkin, Functionalized pentacene: improved electronic properties from control of solid-state order. *J. Am. Chem. Soc.* **123**, 9482-9483 (2001).
- [23] C. M. Hansen, Hansen Solubility Parameters: A User's Handbook, 2nd ed., CRC Press, Boca Raton (2007).
- [24] B.S. Ong, Y.L. Wu, P. Liu, Design of High-Performance Regioregular Polythiophenes for Organic Thin-Film Transistors, *Proc. IEEE*, **93**, 1412-1419 (2005).
- [25] K.Takazawa, Y.Kitahama, Y.Kimura, G.Kido, Optical waveguide self-assembled from organic dye molecules in solution, *Nano Lett.* **5**, 1293-1296 (2005).
- [26] W.H. Lee, D.H. Kim, Y. Jang, J.H. Cho, M. Hwang, Y.D. Park, Y.H. Kim, J.I. Han, K. Cho, Effects of the permanent dipoles of self-assembled monolayer-treated insulator surfaces on the field-effect mobility of a pentacene thin-film transistor, *Appl. Phys. Lett.*, **90**, 132104-132106 (2007).
- [27] B. Akkerman, H. Li, Z. Bao, Fabrication of organic semiconductor crystalline thin films and crystals from solution by confined crystallization, *Organic Electronics* **13**, 235-243 (2012).
- [28] C. Pitsalidis, N. Kalfagiannis, N. A. Hastas, P. G. Karagiannidis, C. Kapnopoulos,, A. Ioakeimidis and S. Logothetidis, High performance transistors based on the controlled growth of triisopropylsilylethynyl-pentacene crystals *via* non-isotropic solvent evaporation, *RSC Adv.* **4**, 20804-20813 (2014).

Figure captions

Figure 1. UV/Vis absorption spectra of TIPS-pentacene dissolved in different anisole/decane solvent mixtures at a constant 1×10^{-5} M. Arrows illustrate the blue shift with increasing decane content.

Figure 2. TIPS-pentacene as a function of anisole/decane wt-% ratio. (a) pure anisole, (b) anisole/decane 96/4 wt-%, (c) anisole/decane 90/10 wt-%. Top: Optical image with the golden areas showing vacuum-deposited gold electrodes, channel length 60 μm . Middle: AFM images for which the numbered sections are shown in the corresponding bottom panel.

Figure 3. The surface roughness on top of terraces of TIPS-pentacene for (a) varying composition of anisole/decane binary solvent on silicon (b) varying aPS concentration for 93/7 wt-% anisole/decane solvent on silicon (c) the same conditions as (b) for films deposited onto PVP-treated silicon.

Figure 4. AFM images (5 μm scan size) of TIPS-pentacene blended with aPS drop cast from 93/7 wt-% anisole/decane on SiO_2 at 30 $^\circ\text{C}$ (a) 5 wt-% aPS, (b) 10 wt-% aPS, (c) 15 wt-% aPS and (d) 20 wt-% aPS.

Figure 5. AFM images of pure and blended TIPS-pentacene from drop casted from 93/7 wt-% anisole/decane on PVP at 30 $^\circ\text{C}$. (a) pure TIPS-pentacene, (b) 5 wt-% aPS, (c) 10 wt-% aPS, (d) 15 wt-% aPS, (e) 20 wt-% aPS.